Stable isotope patterns in micronekton from the Mozambique Channel

Frédéric Ménard, Hermann Doris Benivary, Nathalie Bodin, Nathalie Coffineau, François Leloc'H, Thomas Mison, Pierre Richard, Michel Potier

1 **Stable isotope patterns in micronekton from the Mozambique Channel**

2 Frédéric Ménard[a,*], Herman Doris Benivary[b], Nathalie Bodin[a], Nathalie Coffineau[a], François

3 Le Loc'h[a], Thomas Mison[a], Pierre Richard[c], Michel Potier[a]

4 [a] Institut de Recherche pour le Développement (IRD), UMR 212 EME (IRD/IFREMER/UM2),

5 Avenue Jean Monnet, BP 171, 34203 Sète cedex, France

6 [b] Institut Universitaire de Science de l'Environnement et de Santé, Université d'Antsiranana,

7 Antsiranana 20, BP 0, Madagascar

8 [c] UMR 7266 CNRS-Université de La Rochelle, 2 rue Olympe de Gouges, 17000 La Rochelle,

9 France

10 * Corresponding author

11 frederic.menard@ird.fr

12 Tel +33(0)4 99 57 32 30

13 Fax +33(0)4 99 57 32 95

14

ABSTRACT

We measured the stable carbon ($\delta^{13}C$) and nitrogen ($\delta^{15}N$) isotopic composition of tissues of micronektonic organisms (fishes, squids, crustaceans and gelatinous organisms) collected in the Mozambique Channel during two scientific cruises in 2008 and 2009. The oceanic circulation in the Mozambique Channel is dominated by mesoscale cyclonic and anticyclonic eddies which play a key role in biological processes of less-productive deep-sea ecosystems. We investigated the potential impact of mesoscale features on the $\delta^{13}C$ and $\delta^{15}N$ values of 32 taxa of micronekton. Fishes, squids, crustaceans and gelatinous organisms encompassed a wide range of isotopic niches, with large overlaps among species. Our results showed that mesoscale features did not really influence the isotopic signatures of the sampled organisms, although cyclonic eddies can occasionally impact the nitrogen signatures of micronekton. We show that $\delta^{13}C$ values were intermediate between standard offshore and nearshore signatures, suggesting that pelagic production in the Mozambique Channel could be partly supported by the transport and export of inorganic and organic particles from the Mozambican coast toward the offshore area. Trophic levels calculated from $\delta^{15}N$ values ranged from 2.6 to 4.2, showing that micronekton taxa can be tertiary consumers in the Mozambique Channel. Our findings evidenced clusters of micronektonic organisms according to their $\delta^{15}N$ or $\delta^{13}C$ isotopic signatures, but variations in stable isotope values reflect a complex set of embedded processes linked to physical mesoscale dynamics (rotational dynamics of eddies) and basic biology and ecology of micronektonic organisms (vertical habitat, migration pattern, dietary habits, body length) that are discussed with regard to the stable isotope method based on time-integrated assimilated food.

KEYWORDS: Micronekton, $\delta^{13}C$, $\delta^{15}N$, Mesoscale, Oceanic eddies, Diel vertical migration, Trophic level, Mozambique Channel.

1. INTRODUCTION

The circulation in the Mozambique Channel (south-west Indian Ocean) is ruled by an important mesoscale activity (de Ruijter et al., 2002). Mesoscale rotating eddies propagate southwards along the western edge of the channel (Quartly and Srokosz, 2004; Schouten et al., 2003). These mesoscale features contribute to ocean mixing processes and consequently impact the biological activity at different scales. Cyclonic eddies (clockwise rotating in the southern hemisphere) generate vertical pumping of nutrients in their centres (Bakun, 2006; Chelton et al., 2011; McGillicuddy Jr et al., 1998), enhancing local primary production (Benitez-Nelson et al., 2007; Mizobata et al., 2002; Tew-Kai and Marsac, 2009). On the opposite, anticyclonic eddies (counter-clockwise rotating) are usually associated with low chlorophyll levels (Bakun, 2006; Chelton et al., 2011). However, phytoplankton enrichment has also been associated with the upward movement of nutrient rich waters at the edges of either cyclonic or anticyclonic eddies (Mizobata et al., 2002; Quartly and Srokosz, 2004). In addition, coastal primary production produced on the western side of the channel can be horizontally advected by continuous contra-rotating eddy pairs, referred to as dipoles and propagating southwards (Roberts et al., this issue; Ternon et al., this issue). By influencing the horizontal and vertical distribution at the base of the food web (nutrients, phytoplankton and zooplankton), these features have been suggested to alter the distribution of intermediate trophic links such as micronekton, and thus the distribution of upper-trophic level organisms.

Biological responses to mesoscale eddies have been documented for mesozooplankton and fish larvae (Bakun, 2006; Muhling et al., 2007), for tunas and swordfish (Young et al., 2001);(Seki et al., 2002), for turtles (Lambardi et al., 2008; Polovina et al., 2004), for seabirds (Hyrenbach et al., 2006; Nel et al., 2001; Weimerskirch et al., 2004), or for marine mammals (Bailleul et al., 2010). In spite of their importance, the impact of mesoscale features on micronektonic organisms remains fragmented and is still poorly quantified (see Potier et al., this issue). Recent investigations showed that eddies can shape the distribution and the aggregation patterns of micronekton through bottom-up processes (Drazen et al., 2011; Sabarros et al., 2009). Micronekton refers to small, but actively swimming, organisms (*ca.* 1 to 20cm), mainly crustaceans, fishes, and squids, that form the link between zooplankton and large fish predators in open-sea ecosystems (Brodeur and Yamamura, 2005; Potier et al., 2007). Most of micronekton performs large diel vertical migrations during the crepuscular periods (dawn and dusk), from depths below 400m during the day to the surface layers at night (Benoit-Bird et al., 2009).

In this work, we analyzed the ratios of stable carbon ($\delta^{13}C$) and nitrogen ($\delta^{15}N$) isotopes in the tissues of micronektonic organisms collected in the Mozambique Channel within the framework of the MESOBIO programme (Ternon et al., this issue). Carbon and nitrogen isotopes have often successfully been applied to investigate foraging ecology and trophic relationships in marine ecosystems (Cherel et al., 2010; Fanelli et al., 2011; Ménard et al., 2007; Olson et al., 2010; Revill et al., 2009; Stowasser et al., 2012). Stable isotope ratios of carbon and nitrogen in consumer tissues reflect those of their prey in a predictable manner, and depend on the isotopic signature at the base of the food web (Fry, 2006; Post, 2002). The $\delta^{15}N$ values mainly estimates the relative trophic position of an animal thanks to predictable enrichment of ^{15}N with increasing trophic level (Vanderklift and Ponsard, 2003).

Thus, $\delta^{15}N$ has been used for quantifying and comparing trophic levels of consumers (Cherel et al., 2008). By contrast, $\delta^{13}C$ variations are used to determine the sources of primary production, inshore versus offshore or pelagic versus benthic contribution to food intake (Rubenstein and Hobson, 2004). Different processes affect isotopic baselines of $\delta^{13}C$ and $\delta^{15}N$, including nutrient source, primary productivity, depth and ocean mixing processes (Fry, 2006). The present work aims (1) to investigate the potential impact of mesoscale features on the ratios of stable carbon and nitrogen isotopes of micronektonic organisms, and (2) to interpret the isotopic niches and the trophic levels of micronektonic species in the Mozambique Channel.

2. MATERIAL AND METHODS

2.1. Sample collection

Micronekton samples were collected from two scientific cruises during December 2008 on board R/V Fridtjof Nansen (2008 ASCLME survey n°4, called hereafter MC08A) and during November 2009 on board R/V ANTEA (referred to as MC09B). A Young Gadoid Pelagic Trawl (YGPT) was used during MC09B with a cod-end lined with 5mm knotless nylon delta mesh netting, while an Akrahamn pelagic trawl with cod-end 10mm was used during MC08A. Trawls were conducted during the day on aggregations detected by acoustics, and during the night at the surface on sound scattering layers (0-200m). Night trawl depth was selected according to highest acoustic detections. Each trawl was towed for 30 min at a speed of 3 to 4 knots. A total of 16 and 18 trawls were performed during MC08A and MC09B, respectively (from which 2/3 were carried out at nighttime). The whole catch was sorted and soft tissues of selected micronekton species were removed for further isotopic analyses: dorsal muscle for fishes, mantle for squids, abdomen for crustaceans and body wall for pelagic gastropods

molluscs, siphonophorans, leptocephali larvae and salps. Body length of each individual was measured except for salps: standard length (SL) for fishes, dorsal mantle length (DML) for squids, cephalothorax length (CT) for crustaceans, and total length for the other taxa.

2.2. Stable isotope analysis

Samples were freeze-dried and ground to a fine homogeneous powder. Since lipids are depleted in ^{13}C, lipids were removed using dichloromethane on an accelerated solvent extraction system (ASE®, Dionex;(Bodin et al., 2009). This method does not alter $\delta^{15}N$ signatures. The extent of lipid extraction was checked through the C/N mass ratio of the samples (Post et al., 2007). Lipid-free samples were dried at 50°C before processing, and then 300 to 400 µg of homogenized powder were packed into 8 × 5mm tin containers. Isotopic ratios were determined by a continuous flow mass spectrometer coupled on line to an elemental analyzer. Replicate measurements of internal laboratory standards indicated measurement errors less than 0.15‰ and 0.20‰ for $\delta^{13}C$ and $\delta^{15}N$, respectively. Triplicate measurements performed on some samples confirmed that analytical reproducibility was very good (0.2‰ maximum variation). Isotopic ratios are expressed in the conventional δ notation as parts per thousand (‰) deviations from the international standards: atmospheric nitrogen (N_2) for $\delta^{15}N$ and VPDB Belemnite for $\delta^{13}C$.

$$\delta X = (R_{sample}/R_{standard} - 1) \times 1000 \quad (1)$$

where X is ^{15}N or ^{13}C, R is the corresponding ratio $^{15}N/^{14}N$ or $^{13}C/^{12}C$.

2.3. Data analysis

Satellite altimetry allows identification of mesoscale features (Chelton et al., 2007). One mesoscale feature among five classes (anticyclone, A; cyclone, C; divergence, D; front, F; and

133 shelf station, S) was assigned to each of the 34 trawling stations. The classification of each
134 individual station was processed using three explanatory variables (sea level anomaly,
135 geostrophic speed and bathymetry) and a discriminant function estimated from an extra
136 training dataset (Lamont et al., this issue). Ocean bathymetry was extracted from ETOPO1
137 Global Topography (data access: http://www.ngdc.noaa.gov/mgg/global/global.html). Sea
138 level anomaly and the corresponding geostrophic speed were extracted from AVISO
139 products "DT-MSLA Ref" (Delayed Time, DT; Reference, "Ref") with 0.33 × 0.33° spatial
140 resolution on a Mercator grid. The predictions from the linear discriminant analysis were
141 estimated for each station using the values taken by the three explanatory variables at the
142 corresponding temporal and spatial positions.
143 Links between isotope values ($\delta^{15}N$ and/or $\delta^{13}C$), and broad categories and mesoscale
144 features were investigated using multivariate analysis of variance (MANOVA), Kruskal-Wallis
145 (KW) non-parametric tests and univariate regression tree (URT). URT is a powerful statistical
146 tool that explains the variation of a single response variable ($\delta^{15}N$ or $\delta^{13}C$) using several
147 explanatory variables by growing a tree that partitions the data set into mutually exclusive
148 groups (Venables and Ripley, 2002). The objective is to partition the response into
149 homogeneous groups. All the data are represented by a single node at the top of the tree.
150 Then the tree is built by repeatedly splitting the data. Each split is defined by a simple rule
151 based on a single explanatory variable. Splits are chosen to maximize the homogeneity of
152 the resulting two nodes. However, the splitting procedure grows an overlarge tree. To keep
153 the tree reasonably small, a prune back procedure is applied. Each final group is
154 characterized by mean values of $\delta^{15}N$ or $\delta^{13}C$.

As the content of ^{15}N in animal tissues is biomagnified along the length of a food chain (Post, 2002), trophic levels (*TL*) of micronekton taxa were calculated on the basis of isotopic measurements using the following equation:

$$TL = 2.0 + \frac{\delta^{15}N_i - \delta^{15}N_{primary\ \ consumer}}{3.2} \quad (2)$$

where $\delta^{15}N_i$ is the nitrogen isotopic composition of any given micronekton taxon *i*, $\delta^{15}N_{primary\ consumer}$ is the $\delta^{15}N$ reference baseline value at trophic level 2, and 3.2‰ is an estimate of the average increase of $\Delta^{15}N$ per trophic level (Cherel et al., 2010; Sweeting et al., 2007). Using primary consumers as a baseline might reduce error in the estimation of *TL* (Martínez del Rio et al., 2009). Salps are known to be filter-feeders grazing on phytoplankton and other small food items. They were often chosen as the primary consumer species for estimating trophic levels using equation (2) (Cherel et al., 2010, 2008; Stowasser et al., 2012). Therefore, we chose average $\delta^{15}N$ value of *Salpa maxima* as the reference value for the food base. The mean was computed using three $\delta^{15}N$ values (5.0, 5.2, 5.2‰) from MC08A and one (5.2‰) from MC09B.

3. RESULTS

Fig. 1 displays the location of the 34 trawls categorized in four mesoscale feature classes (cyclones C, anticyclones A, fronts F, divergences D and shelf station S). A total of 545 organisms amongst 32 taxa were analyzed (Table 1). Not all micronekton taxa were caught at all mesoscale features, in particular few individuals were collected in anticyclones and cyclones (68 and 77, respectively) compared with those collected in divergences and fronts (187 and 121, respectively).

3.1. Micronekton assemblage

179 Taxa were divided in four broad categories: gelatinous organisms (*Salpa maxima*,
180 siphonophorans, the pelagic gastropod molluscs *Carinaria lamarckii* and leptocephali larvae),
181 crustaceans (*Funchalia* spp., *Oplophorus* sp. and *O. typus*), squids (*Cranchia scabra*,
182 *Ornithoteuthis volatilis*, *Sthenoteuthis oualaniensis*), and fishes. Fishes represented 16
183 species, 5 genera and 1 family. The family Bramidae grouped juveniles of *Pterycombus*
184 *petersii* and of other undetermined species: they were not segregated by both δ^{15}N
185 (Kruskall-Wallis, H = 1.19, $P > 0.27$) and δ^{13}C values (H = 0.43, $P > 0.50$). The *Thunnus* spp.
186 category comprised very small juvenile scombrids that were not identified. *Psenes* spp.
187 comprised 2 species (*P. cyanophrys*, *P. whiteleggii*) that were not segregated by their δ^{15}N
188 signatures (Kruskall-Wallis, H = 1.78, $P > 0.18$), but slightly segregated by δ^{13}C (Kruskall-
189 Wallis, H = 4.0, $P = 0.045$). The genus *Diaphus* is taxonomically one of the most difficult in the
190 family Myctophidae. We accurately identified three species (*D. garmani*, *D. metopoclampus*,
191 *D. richardsoni*). The *Diaphus* spp. category groups other species that were not identified.
192 Juveniles were collected for Bramidae, *Decapterus* sp., *Pterycombus petersii*, *Psenes* spp. and
193 *Thunnus spp* only.
194 Means of C/N mass ratio encompassed a narrow range (between 3.0 and 3.4 for 30 taxa;
195 only *Salpa maxima* and leptocephali larvae had ratios greater than 4; Table 1). Such small
196 values indicated low lipid content after lipid removal, thus allowing accurate comparisons of
197 δ^{13}C values among sample types. Isotopic analyses revealed a considerable range of δ^{13}C and
198 δ^{15}N mean values, 3.3 and 6.9‰, respectively. The δ^{13}C mean values ranged from –20.6 $\pm$
199 0.57‰ (letocephal larvae) to –17.3 $\pm$ 0.24‰ (*Oplophorus* sp.) (Table 1). The δ^{15}N ranged
200 from 5.2 $\pm$ 0.11‰ (*Salpa maxima*) to 12.1 $\pm$ 0.44‰ (*Diaphus metopoclampus*).
201 The four broad categories (fishes, squids, crustaceans and gelatinous organisms) were
202 segregated by their isotope signatures of both nitrogen and carbon treated as a multivariate

response (MANOVA, Wilk's lambda, $F_{3,540}$ = 58.37, *P < 0.0001*). They were also segregated in their isotopic signatures in both $\delta^{13}C$ (univariate analysis, KW test, *H* = 115.0, *P < 0.0001*; pairwise comparisons indicated that crustaceans and squids were not significantly different) and $\delta^{15}N$ values (KW test, *H* = 56.0, *P < 0.0001*; fishes and squids did not differ significantly). Fig. 2 displays a summary of $\delta^{13}C$ and $\delta^{15}N$ values (mean $\pm$ standard deviation) of all the taxa grouped by broad categories. To give a better picture of the trophic structure of the assemblages, taxa of the four broad categories were placed in sequence according to their nitrogen and carbon mean values (Fig. 3a and 3b, respectively). Tests were then conducted by categories:

- The 22 taxa of fish were segregated by their overall isotopic signatures (MANOVA, Wilk's lambda, $F_{21,354}$ = 14.99, *P < 0.0001*), and both $\delta^{13}C$ (KW test, *H* = 151.1, *P < 0.0001*) and $\delta^{15}N$ values (KW test, *H* = 249.6, *P < 0.0001*). The most enriched values were found for known deep migrating mesopelagic fishes such as several Myctophidae (all of the genus *Diaphus*, *Lobianchia gemellarii*), the bregmacerotid *Bregmaceros macclellandii*, the notosudid *Scopelosaurus hoedti*, and the sternoptychid *Argyropelecus aculeatus*. *Cubiceps pauciradiatus* (Nomeidae) and *Decapterus* sp. (Carangidae) exhibited large standard deviations of $\delta^{15}N$ thanks to a subset of specimens caught in one cyclone of MC09B with very high $\delta^{15}N$ values (see below).

- Overall isotopic signatures differed between the three squid species (MANOVA, Wilk's lambda, $F_{2,101}$ = 4.90, *P < 0.001*), but only the KW test based on $\delta^{13}C$ signatures was significant (*H* = 10.62, *P < 0.005* for $\delta^{13}C$; *H = 0.85*, *P = 0.66* for $\delta^{15}N$).

- For crustaceans (three taxa) and gelatinous organisms (four taxa), multi- and univariate tests were all significant. Standard deviations of both $\delta^{13}C$ and $\delta^{15}N$ for leptocephali larvae were very high, while the nitrogen signatures of *Salpa maxima* varied very little (5.2 $\pm$

227 0.11‰). *Oplophorus typus* (crustacean) was the only non-fish taxa having a $\delta^{15}N$ average
228 greater than 10.0‰ (Fig. 3a), and *Oplophorus* sp. had the most ^{13}C enrichment.
229
230 **3.2. Impact of mesoscale features**
231 No clear pattern emerged from $\delta^{13}C$ *vs.* $\delta^{15}N$ bi-plots of the 545 individuals categorized by
232 broad category and by mesoscale feature (figures not shown). To investigate the structure of
233 the data and assess the influence of eddies, we conducted univariate regression tree
234 analyses (URT) on $\delta^{15}N$ and $\delta^{13}C$ values using cruise, broad category, mesoscale feature,
235 taxon and body length as covariates. Five groups were identified by the URT based on $\delta^{15}N$
236 values (Fig. 4a). Groups were sorted in order of increasing $\delta^{15}N$ predicted values (Fig. 4b).
237 The first splits of the pruned tree separated taxa: one group of low $\delta^{15}N$ values clustered
238 gelatinous organisms (except siphonophorans), small fishes and one crustacean (*Funchalia*
239 *spp*.); the other group put together deep migrating mesopelagic organisms (11 fish taxa and
240 the crustacean *Oplophorus typus*) with rather high $\delta^{15}N$ values. A further split separated
241 cyclonic eddies from the four other classes (anticyclones, divergences, fronts and shelf
242 stations). The non cyclonic group mixed taxa from the four broad categories. The “cyclonic”
243 branch of the pruned tree separated two groups (Fig. 4a and 4b): *Cyclonic 1* grouped 22
244 individuals (14 fishes, three specimens of the crustacean *Oplophorus* sp. and five specimens
245 of the squid *Cranchia scabra*) with intermediate $\delta^{15}N$ values (predicted value of 9.4‰);
246 *Cyclonic 2* clustered six specimens of *Cubiceps pauciradiatus* (fish) and one *Ornithoteuthis*
247 *volatilis* (squid) collected in the same cyclone sampled in November 2009 (cruise MC09B),
248 with the highest $\delta^{15}N$ values (predicted value of 14.1‰).
249 Four groups were identified by the URT based on $\delta^{13}C$ values. Taxon was the only significant
250 covariate used to develop the pruned tree (Fig. 5a and 5b). Group 2 clustered most of the

micronekton taxa (Fig. 5a and 5b) with a predicted average of –18.7‰. Group 3 classified taxa with the highest ^{13}C enrichment (predicted $\delta^{13}C$ value of –18.2‰). Leptocephali larvae were segregated owing to their low $\delta^{13}C$ values.

3.3 Trophic levels and size

Since size is an important factor structuring trophic links, we looked at the potential relationships between body length and $\delta^{15}N$ values. However we were limited by sample sizes and body length ranges, and size effect was tested for ten taxa only (Table 1). The fishes Bramidae, *Cubiceps pauciradiatus*, *Thunnus* spp. and the squid *Sthenoteuthis oualaniensis* showed a significant body length effect (Fig. 6 and Table 2). One outlier for *S. oualaniensis* was removed from the linear regression (Fig. 6b). Fig. 6c reveals that a simple model was not appropriate for *C. pauciradiatus*: the six individuals sampled in the cyclone of November 2009 were cut off from the other individuals. The final model did not select two separate linear regressions. The most parsimonious model retained parallel regressions (same estimated slope) and different intercepts (Table 2).

Estimated TLs within the micronekton consumers of Mozambique Channel ranged from 2.2 (leptocephali larvae) to 4.2 (the fish *D. metopoclampus*), encompassing theoretically two trophic levels (Table 1). Of course, estimated TLs exhibited the same patterns as $\delta^{15}N$ values because the only unknown in equation (2) was the nitrogen isotopic composition of micronekton taxa. The three squid species shared the same TL (3.3 to 3.4), and the deep migrating mesopelagic fishes and the crustacean *O. typus* had the highest TLs.

4. DISCUSSION

To our knowledge this study is the first that investigates the potential impact of mesoscale eddies on the isotopic signatures of a large assemblage of micronekton from gelatinous organisms to fish. An extensive investigation conducted on two counter-rotating eddies off Western Australia analyzed mainly the impact of eddies on the isotopic composition of dissolved inorganic nitrogen, particulate organic matter and mesozooplankton (Waite et al., 2007). Fish larvae identified at the family level were also collected with small nets, allowing the analysis of eel leptocephals and of small-sized specimens of Myctophidae, Sternoptychidae, Paralepididae, Phosichthyidae and Scorpaenidae only. The results of Waite et al. (2007) showed no significant difference in the $\delta^{15}N$ signature between the fish larvae from the two eddies, but myctophid larvae from the warm-core eddy (i.e., counter-clockwise rotational sense) are significantly enriched in ^{13}C relative to those from the cold-core eddy (i.e., cyclonic rotation). In our study, the fish taxa sampled covered several main open-ocean micronekton fish families (juveniles and/or adults) found in the Mozambique Channel: Myctophidae, Nomeidae, Bramidae, Phosichthyidae, Sternoptychidae, Notosudidae, Gonostomatidae, Paralepididae, Bregmacerotidae and Carangidae. Our findings showed that mesoscale features did not have any clear impact on the carbon and nitrogen signatures of micronekton in the Mozambique Channel. The 32 taxa of crustaceans, squids and fishes encompassed a wide range of isotopic niches, with large overlaps among species. Regression trees evidenced patterns with clusters of organisms according to their $\delta^{15}N$ or $\delta^{13}C$ isotopic signatures. We attempt henceforward to examine some hypotheses supported by our results, taking into account the nature of our data and the stable isotope method.

4.1 Isotopic patterns amongst mesoscale features

297 Eddies play a key role in biological processes of less-productive deep-sea ecosystems by
298 converting physical energy into trophic energy (Bakun, 2006; Godø et al., 2012). They have
299 been suggested to impact the distribution of marine organisms through bottom-up effects
300 (Domokos, 2009; Domokos et al., 2007; Drazen et al., 2011; Muhling et al., 2007; Sabarros et
301 al., 2009; Seki et al., 2002; Tew Kai and Marsac, 2010). On the one hand few individuals in
302 our study had their δ^{15}N values directly impacted by mesoscale features which on the other
303 hand did not influence the carbon signatures of the sampled organisms. Six specimens of the
304 nomeid *C. pauciradiatus* and one *O. volatilis* (Ommastrephidae) were grouped by the
305 regression tree based on their δ^{15}N values (*Cyclonic 2*, Fig. 4). These specimens were
306 collected in the same cyclone sampled in November 2009 during the MC09B cruise, and had
307 distinctly higher δ^{15}N signatures than their congeners sampled in other mesoscale features.
308 Surprisingly, specimens from other species or taxa (leptocephali larvae, the squid *Cranchia*
309 *scabra*, the crustacean *Funchalia* spp., and the fishes *Argyropelecus aculeatus*, *Hygophum*
310 *hygomii* and *Vinciguerria nimbaria*) collected in the same cyclone did not show a similar
311 pattern. Their δ^{15}N signatures did not differ significantly from specimens collected in other
312 features (all KW test had a *p*-value much greater than 10%). This singular pattern could
313 suggest possible residency for the nomeid *C. pauciradiatus* into the eddy, while other species
314 or taxa could move among the water masses. Lamkin (1997) showed indeed that adult
315 spawning grounds and larval habitat of *C. pauciradiatus* can be tied to frontal systems along
316 eddy rings in the Gulf of Mexico. Mesoscale features impacted the nitrogen signatures of
317 *Thunnus* spp. only, with higher δ^{15}N signatures within anticyclones (KW test, $H = 15.0$, $P < 0.001$). Two extra individuals sampled in the same cyclone could have been added to the
319 *Cyclonic 2* group: one *Decapterus* sp. which had the highest δ^{15}N value (16.6‰) and one
320 *Lobianchia gemellarii* (δ^{15}N = 12.4‰). In cyclonic eddies, vertical fluxes of nitrate can

dominate production leading to higher $\delta^{15}N$ signatures of the phytoplankton compared with an anticyclonic eddy, where nitrate supply to the surface could be physically limited (Bakun, 2006; McGillicuddy Jr and Robinson, 1997; Muhling et al., 2007; Waite et al., 2007). To impact the isotopic signature of pelagic consumers such as micronekton organisms, one should assume that this isotopic baseline is incorporated and conserved through several trophic levels trapped in the water mass of the cyclonic eddy. However this hypothesis is challenged by the ecology and behaviour of micronekton organisms.

The vast majority of micronekton organisms typically occurs in the surface layer during the night and migrates below 400m depth during the day (Behagle et al., this issue). Micronekton ascents and descents during the crepuscular periods (dawn and dusk) characterize this process of diel vertical migration (Benoit-Bird et al., 2009). In the Humboldt Current system, the vertical extent of the water mass trapped in eddies has been recently estimated to 240m and 530m in cyclonic and anticyclonic eddies respectively, with a global decrease of the physical gradients with depth (Chaigneau et al., 2011). These estimates are most likely variable from eddy to eddy and from one area to another. In eddies of the Mozambique Channel, swirl velocities are weaker in deeper layers than they are at the surface (Ternon et al., this issue). In addition, Kolasinski et al. (2012) showed that physico-chemical characteristics of deep waters (including carbon and nitrogen isotopic values of POM) from cyclonic and anti-cyclonic eddy of the Mozambique Channel were alike. Consequently, the diel vertical migration causes micronekton to stay half of the time in water masses weakly impacted by eddies. Contrary to the study of Godø et al. (2012) in the Norwegian Sea, we believe that horizontal structure is not preserved during diel vertical migration in the Mozambique Channel: migration did not take place in accordance with the

345 water mass trapped in eddies. In addition, eddies are translated rather slowly in the
346 Mozambique Channel (5.2cm.s^{-1}; (de Ruijter et al., 2002) while the average speed of a
347 mesopelagic fish was measured acoustically to be about 30cm.s^{-1} (Torgersen and Kaartvedt,
348 2001). Therefore, fish and most likely squids would still have the ability to swim across
349 eddies at any depth. However very few studies investigated how crustaceans swim. Morris
350 et al. (1985) analyzed the swimming in a small calanoid copepod (*Pleuromamma xiphias*,
351 6mm): they estimated maximal velocities to be 0.3m.s^{-1} during the power strokes of an
352 entire swimming cycle, and less than 0.1m.s^{-1} during the recovery strokes. The total lengths
353 of the three crustacean taxa in our study are at least five times the size of *P. xiphias* and
354 maximal swimming velocity scales with body length. We thus believe that micronekton is
355 rarely trapped in the water mass of a particular eddy and thus does not necessarily feed on
356 concentrations of zooplankton prey found in the eddy only.
357
358 Isotopic incorporation in animal tissues is linked to turnover rates that vary according to
359 tissue, body size, growth or taxon (Martínez del Rio et al., 2009). The dynamics of isotopic
360 incorporation can then blur the interpretation of our field isotopic measurements. Indeed, a
361 sampled micronekton specimen that had recently moved into an eddy from surrounding
362 waters may have had a previous $\delta^{15}N$ or $\delta^{13}C$ signature that would have been gradually
363 modified as they fed on new food sources trapped in the eddy. Depending on tissue-specific
364 isotopic turnover, stable isotope measurements reflect average dietary records over days
365 (e.g, whole fish larvae; Herzka and Holt, 2000) to years (e.g., elasmobranch muscle; MacNeil
366 et al., 2006; Logan and Lutcavage, 2010). No clear studies estimated isotopic turnovers for
367 micronekton but several weeks seem a reasonable order of magnitude. Consequently, the

368 particular isotope baseline of an eddy is likely not conserved through these pelagic
369 consumers.
370
371 However, migration can be a multifaceted and plastic response of micronekton. Partial diel
372 vertical migration has been reported in the literature, showing that resident and migrant
373 strategies can co-exist in some populations (Mehner and Kasprzak, 2011; Olsson et al.,
374 2006). In addition several taxa in our data were clearly epipelagic (leptocephali larvae, *Salpa*
375 *maxima*, *Thunnus* sp., *Decapterus* sp.). Notwithstanding their swimming abilities and
376 assuming a passive transport, all these species would then be more sensitive to eddy
377 structure. If trapped in the water mass of the eddy, they can prey on local concentrations of
378 zooplankton propagating the baseline of the "eddy" isotopic signature. This scenario might
379 be true for the specimens of the grouping *Cyclonic 2*.
380
381 **4.2 Carbon isotope patterns**
382 There was no significant difference in $\delta^{13}C$ signatures of micronekton between mesoscale
383 features. The $\delta^{13}C$ values ranged from –20.6 to –17.3‰ suggesting that micronekton
384 organisms sampled exploit different sources of primary production, giving rise to different
385 trophic pathways. However, most of $\delta^{13}C$ mean values encompassed a narrow range
386 between –19 and –18‰ (all squids, 19 fish taxa, two crustacean genera, Fig. 4b). Only
387 gelatinous organisms and three fishes (*Psenes* spp., *Diaphus metopoclampus* and
388 *Pterycombus petersii*) were depleted in ^{13}C compared with the other taxa. Leptocephali
389 larvae which could feed on detritical materials and fecal pellets (Lecomte-Finiger et al., 2004)
390 had the most ^{13}C-depleted carbon signature with a large variance of $\delta^{13}C$ values too.
391 Surprisingly, our $\delta^{13}C$ values were intermediate between standard offshore pelagic

signatures and nearshore signatures measured in this region (Hill et al., 2006; Kolasinski et al., 2012), suggesting that pelagic production in the Mozambique Channel could be partly supported by the transport and export of inorganic and organic particles from the Mozambican coast toward offshore area, through the "vacuum-cleaner effect" due to rotational dynamics of eddies (Tew-Kai and Marsac, 2009).

4.3 Trophic levels of micronekton

Micronekton form a key trophic link between top predators and zooplankton (Brodeur and Yamamura, 2005), and are theoretically assumed to constitute the tertiary level of pelagic food webs. The lowest trophic level except salps was occupied by leptocephali larvae (TL = 2.2), and TLs less than 3.0 were estimated for the carnivorous heteropod *Carinaria lamarckii*, the penaeids *Funchalia* spp. and juveniles of three fish taxa (*Thunnus* spp., *Pterycombus petersii* and *Psenes* spp.). The remaining estimated TLs encompassed a continuum of values between 3.1 and 4.2, very close to those obtained by Cherel et al. (2010) and Stowasser et al. (2012) for myctophids in the Southern Ocean. Our results show that micronekton sampled can occupy relatively high trophic positions: the high TL of the myctophid *Diaphus metopoclampus* probably fits with a diet based on euphausiids or small fish larvae, and the high TL of the crustacean *Oplophorus typus* is explained by a diet strongly dominated by detritus (Karuppasamy and Menon, 2004), which are known to be ^{15}N-enriched. However our organisms were preying upon a similar range of herbivorous and omnivorous consumers, mainly meso- or macrozooplankton.

Body size is known to play a crucial role in predator–prey interactions (Sheldon et al., 1977). Body length can influence δ^{15}N values (then TL) of one species because larger specimens can

416 catch larger prey as they grow (e.g. Parry, 2008). However intraspecific variation in $\delta^{15}N$ with
417 body length was identified in three fish taxa and one squid species only (Fig. 6 and Table 2).
418 For these taxa, the positive significant relationships may be indicative of larger specimens
419 feeding at higher trophic levels. We probably cannot conclude for the other taxa as pelagic
420 trawls used for sampling micronekton selected limited size ranges for each species (Table 1).
421 Interestingly, a model with two intercepts and one slope was fitted to the data of the fish
422 *Cubiceps pauciradiatus*. The common slope may be indicative of consistent ontogenetic
423 variability (i.e. a similar intraspecific variation), while different intercepts can result from a
424 shift in habitat use (i.e., $\delta^{15}N$ values impacted by a baseline change in a cyclonic eddy).
425 Furthermore the linear relationship between TL and body length means of taxa was not
426 significant ($F_{1,28}$ = 1.95, P = 0.17 for 30 taxa), showing that the structuring effect of size was
427 not depicted in our data with regard to the range of the body length averages (Table 1).
428 Leptocephali larvae were indeed an outlier in the dataset (very low TL associated with high
429 body length) and salps were unfortunately not measured onboard.
430
431 But the interpretation of trophic level estimated from $\delta^{15}N$ values presents caveats. Isotopic
432 baseline can vary from year to year and can be conserved through several trophic levels.
433 Three salp samples were collected in December 2008 (MC08A) and one in November 2009
434 (MC09B) only, preventing statistical comparison. However $\delta^{15}N$ values were very close and
435 year effect (a confounding variable with the cruise factor which was one covariate in the
436 regression tree) was never significant. In addition sources of variation of the discrimination
437 factor are numerous (Martinez del Rio et al., 2009). These biases in isotopic TL calculation
438 can alter our estimates. In addition, the basic biology and ecology of micronekton

(ontogenetic migration, feeding habits) remain poorly known, making interpretation difficult.

4.4. Limitations of the data

The spatial and temporal resolutions of our isotope data are limited by the sampling coverage of the pelagic trawls that were carried out during two cruises. The two surveys did not sample the same patterns of mesoscale eddies. In 2009 (MC09B), mesoscale features were very stable and well established compared to 2008 (MC08A), where eddies were in their early phases (Ternon et al., this issue). Contrary to Waite et al. (2007) who investigated extensively the same dipole in one area, we sampled mesoscale features at different maturation phases. Eddies are characterized by their dimension, intensity (e.g., sea surface height, geostrophic and rotational velocities), lifetime, origin, trajectory, and propagation distance (Bakun, 2006; Chelton et al., 2011). In addition eddies develop over time scales of weeks to months while biological responses such as diel vertical migration can occur within a day. All these eddy properties and development phases shape biological responses and then impact the stable isotope signatures of the organisms.

In summary, biogeochemical and biological responses to mesoscale dynamics along the food chain up to mid-trophic levels such as micronekton are variable and the underlying mechanisms are complex to disentangle. The stable isotope method, based on time-integrated assimilated food, allowed us to better depict the trophic relationships in this micronekton assemblage. Some species had distinct isotopic niches, but others showed strong overlap. In addition isotopic differences attributed to mesoscale dynamics were evidenced for individuals of the same species. Thus the variations in stable isotope values in

463 our data reflect a complex set of embedded processes linked to physical mesoscale dynamics
464 and basic biology and ecology of micronektonic organisms (e.g. vertical habitat, migration
465 pattern, dietary habits and body length).
466
467 **ACKNOWLEDGEMENTS**
468 This work was mainly supported by the MESOBIO project which was funded by WIOMSA
469 (MASMA grant 2009-2011). IRD (France), Department of Environment Affairs (South Africa),
470 ASCLME, and SWIOFP also participated to the funding of surveys or research works. HDB was
471 granted by IRD, the French SCAC in Madagascar and the WIOMSA (MARGII). The authors
472 thank Dominique Dagorne, Hervé Demarcq and Jean-François Ternon for their help in this
473 work. We also thank John Logan and an anonymous reviewer who helped strengthen this
474 manuscript.
475
476 **REFERENCES**
477 Bailleul, F., Cott, C., Guinet, C., 2010. Mesoscale eddies as foraging area of a deep-diving predator,
478 the southern elephant seal. Mar. Ecol. Prog. Ser. 408, 251–264.
479 Bakun, A., 2006. Fronts and eddies as key structures in the habitat of marine fish larvae: opportunity,
480 adaptative response and competitive advantage. Sci. Mar. 70S2, 105–122.
481 Behagle, N., du Buisson, L., Josse, E., Lebourges-Dhaussy, A., Roudeau, G., Ménard, F. (2013).
482 Mesoscale features and micronekton in the Mozambique Channel: an acoustic approach.
483 Deep Sea Res. Part II
484 Benitez-Nelson, C.R., Bidigare, R.R., Dickey, T.D., Landry, M.R., Leonard, C.L., Brown, S.L., Nencioli, F.,
485 Rii, Y.M., Maiti, K., Becker, J.W., Bibby, T.S., Black, W., Cai, W.-J., Carlson, C.A., Chen, F.,
486 Kuwahara, V.S., Mahaffey, C., McAndrew, P.M., Quay, P.D., Rappe, M.S., Selph, K.E.,
487 Simmons, M.P., Yang, E.J., 2007. Mesoscale Eddies Drive Increased Silica Export in the
488 Subtropical Pacific Ocean. Science 316, 1017–1021.
489 Benoit-Bird, K.J., Au, W.W.L., Wisdom, D.W., 2009. Nocturnal light and lunar cycle effects on diel
490 migration of micronekton. Limnol. Ocean. 54, 1789–1800.
491 Bodin, N., Budzinski, H., Le Ménach, K., Tapie, N., 2009. ASE extraction method for simultaneous
492 carbon and nitrogen stable isotope analysis in soft tissues of aquatic organisms. Anal. Chim.
493 Acta 643, 54–60.
494 Brodeur, R.D., Yamamura, O., 2005. Micronekton of the North Pacific. PICES Sci Rep. No. 30, North
495 Pacific Marine Science Organization, Sidney, BC.

Chaigneau, A., Texier, M.L., Eldin, G., Grados, C., Pizarro, O., 2011. Vertical structure of mesoscale eddies in the eastern South Pacific Ocean: A composite analysis from altimetry and Argo profiling floats. J. Geophys. Res. 116, 16 PP.

Chelton, D.B., Schlax, M.G., Samelson, R.M., 2011. Global observations of nonlinear mesoscale eddies. Prog. Ocean. 91, 167–216.

Chelton, D.B., Schlax, M.G., Samelson, R.M., Szoeke, R.A. de, 2007. Global observations of large oceanic eddies. Geophys. Res. Lett. 34, 5 PP.

Cherel, Y., Ducatez, S., Fontaine, C., Richard, P., Guinet, C., 2008. Stable isotopes reveal the trophic position and mesopelagic fish diet of female southern elephant seals breeding on the Kerguelen Islands. Mar. Ecol. Prog. Ser. 370, 239–247.

Cherel, Y., Fontaine, C., Richard, P., Labat, J.-P., 2010. Isotopic niches and trophic levels of myctophid fishes and their predators in the Southern Ocean. Limnol. Ocean. 55, 324–332.

De Ruijter, W.P.M., Ridderinkhof, H., Lutjeharms J.R.E., Schouten, M.W., Veth, C., 2002. Observations of the flow in the Mozambique Channel. Geophys. Res. Lett. 29, 1502.

Domokos, R., 2009. Environmental effects on forage and longline fishery performance for albacore (Thunnus alalunga) in the American Samoa Exclusive Economic Zone. Fish. Ocean. 18, 419–438.

Domokos, R., Seki, M.P., Polovina, J.J., Hawn, D.R., 2007. Oceanographic investigation of the American Samoa albacore (Thunnus alalunga) habitat and longline fishing grounds. Fish. Ocean. 16, 555–572.

Drazen, J.C., De Forest, L.G., Domokos, R., 2011. Micronekton abundance and biomass in Hawaiian waters as influenced by seamounts, eddies, and the moon. Deep Sea Res. Part I 58, 557–566.

Fanelli, E., Cartes, J.E., Papiol, V., 2011. Food web structure of deep-sea macrozooplankton and micronekton off the Catalan slope: Insight from stable isotopes. J. Mar. Syst. 87, 79–89.

Fry, B., 2006. Stable isotope ecology. Springer, New York.

Godø, O.R., Samuelsen, A., Macaulay, G.J., Patel, R., Hjøllo, S.S., Horne, J., Kaartvedt, S., Johannessen, J.A., 2012. Mesoscale Eddies Are Oases for Higher Trophic Marine Life. Plos One 7, e30161.

Herzka, S.Z., Holt, G.J., 2000. Changes in isotopic composition of red drum (Sciaenops ocellatus) larvae in response to dietary shifts: potential applications to settlement studies. Can. J. Fish. Aquat. Sci. 57, 137-147.

Hill, J.M., McQuaid, C.D., Kaehler, S., 2006. Biogeographic and nearshore–offshore trends in isotope ratios of intertidal mussels and their food sources around the coast of southern Africa. Mar. Ecol. Prog. Ser. 318, 63–73.

Hyrenbach, K.D., Veit, R.R., Weimerskirch, H., Hunt Jr., G.L., 2006. Seabird associations with mesoscale eddies: the subtropical Indian Ocean. Mar. Ecol. Prog. Ser. 324, 271–279.

Karuppasamy, P.K., Menon, N.G., 2004. Food and feeding habits of the pelagic shrimp, Oplophorus typus from the deep scattering layer along the west coast of India. Indian J. Fish. 51, 17-24.

Kolasinski, J., Kaehler, S., Jaquemet, S., 2012. Distribution and sources of particulate organic matter in a mesoscale eddy dipole in the Mozambique Channel (south-western Indian Ocean): Insight from C and N stable isotopes. J. Mar. Syst. 96-97, 122-131.

Lambardi, P., Lutjeharms, J.R.E., Mencacci, R., Hays, G.C., Luschi, P., 2008. Influence of ocean currents on long-distance movement of leatherback sea turtles in the Southwest Indian Ocean. Mar. Ecol. Prog. Ser. 353, 289–301.

Lamkin, J. 1996. The Loop Current and the abundance of larval Cubiceps pauciradiatus (Pisces: Nomeidae) in the Gulf of Mexico: evidence for physical and biological interaction. Fish. Bull. 95, 250-266.

Lamont, T., Barlow, R., Morris, T., Van den Berg, M. (2013). Characterisation of mesoscale features and phytoplankton variability in the Mozambique Channel. Deep Sea Res. Part II

Lecomte-Finiger, R., Maunier, C., Khafif, M., 2004. Les larves de leptocéphales, ces méconnues. Cybium 28, 83-95.

Logan, J.M., Lutcavage, M.E., 2010. Stable isotope dynamics in elasmobranch fishes. Hydrobiologia 644, 231-244.

548 MacNeil, M.A., Drouillard, K.G., Fisk, A.T., 2006. Variable uptake and elimination of stable nitrogen
549 isotopes between tissues in fish. Can. J. Fish. Aquat. Sci. 63:345-353
550 Martínez del Rio, C., Wolf, N., Carleton, S.A., Gannes, L.Z., 2009. Isotopic ecology ten years after a call
551 for more laboratory experiments. Biol. Rev. 84, 91–111.
552 McGillicuddy Jr, D.J., Robinson, A.R., 1997. Eddy-induced nutrient supply and new production in the
553 Sargasso Sea. Deep Sea Res. Part I 44, 1427–1450.
554 McGillicuddy Jr, D.J., Robinson, A.R., Siegel, D.A., Jannasch, H.W., Johnson, R., T. D. Dickey, J. McNeil,
555 A. F. Michaels, A. H. Knap, 1998. Influence of mesoscale eddies on new production in the
556 Sargasso Sea. Nature 394, 263–266.
557 Mehner, T., Kasprzak, P., 2011. Partial diel vertical migrations in pelagic fish. J. Anim. Ecol. 80, 761–
558 770.
559 Ménard, F., Lorrain, A., Potier, M., Marsac, F., 2007. Isotopic evidence of distinct feeding ecologies
560 and movement patterns in two migratory predators (yellowfin tuna and swordfish) of the
561 western Indian Ocean. Mar. Biol. 153, 141–152.
562 Mizobata, K., Saitoh, S.I., Shiomoto, A., Miyamura, T., Shiga, N., Imai, K., Toratani, M., Kajiwara, Y.,
563 Sasaoka, K., 2002. Bering Sea cyclonic and anticyclonic eddies observed during summer 2000
564 and 2001. Prog. Ocean. 55, 65–75.
565 Morris, M.J., Gust, G., Torres, J.J., 1985. Propulsion efficiency and cost of transport for copepods: a
566 hydromechanical model of crustacean swimming. Mar. Biol. 86, 283-295.
567 Muhling, B.A., Beckley, L.E., Olivar, M.P., 2007. Ichthyoplankton assemblage structure in two meso-
568 scale Leeuwin Current eddies, eastern Indian Ocean: The Leeuwin Current and its Eddies.
569 Deep Sea Res. Part II 54, 1113–1128.
570 Nel, D.C., Lutjeharms J.R.E., Pakhomov, E.A., Ansorge, I.J., Ryan, P.G., Klages, N.T.W., 2001.
571 Exploitation of mesoscale oceanographic features by grey-headed albatross Thlassarche
572 chrysostoma in the southern Indian Ocean. Mar. Ecol. Prog. Ser. 217, 15–26.
573 Olson, R.J., Popp, B.N., Graham, B.S., López-Ibarra, G.A., Galván-Magaña, F., Lennert-Cody, C.E.,
574 Bocanegra-Castillo, N., Wallsgrove, N.J., Gier, E., Alatorre-Ramírez, V., Ballance, L.T., Fry, B.,
575 2010. Food-web inferences of stable isotope spatial patterns in copepods and yellowfin tuna
576 in the pelagic eastern Pacific Ocean. Prog. Ocean. 86, 124–138.
577 Olsson, I.C., Greenberg, L.A., Bergman, E., Wysujack, K., 2006. Environmentally induced migration:
578 the importance of food. Ecol. Lett. 9, 645–651.
579 Polovina, J.J., Balazs, G.H., Howell, E.A., Parker, D.M., Seki, M.P., Dutton, P.H., 2004. Forage and
580 migration habitat of loggerhead (Caretta caretta) and olive ridley (Lepidochelys olivacea) sea
581 turtles in the central North Pacific Ocean. Fish. Ocean. 13, 36–51.
582 Post, D.M., 2002. Using stable isotopes to estimate trophic position: models, methods, and
583 assumptions. Ecology 83, 703–718.
584 Post, D.M., Layman, C.A., Arrington, D.A., Takimoto, G., Quattrochi, J., Montaña, C.G., 2007. Getting
585 to the fat of the matter: models, methods and assumptions for dealing with lipids in stable
586 isotope analyses. Oecologia 152, 179–189.
587 Potier, M., Marsac, F., Cherel, Y., Lucas, V., Sabatie, R., Maury, O., Ménard, F., 2007. Forage fauna in
588 the diet of three large pelagic fishes (lancetfish, swordfish and yellowfin tuna) in the western
589 equatorial Indian Ocean. Fish. Res. 83, 60–72.
590 Potier, M., Bach, P., Ménard, F., Marsac, F. (2013). Influence of mesoscale features on micronekton
591 and top predators in the Mozambique Channel. Deep Sea Res. Part II
592 Quartly, G.D., Srokosz, M.A., 2004. Eddies in the southern Mozambique Channel. Deep Sea Res. Part
593 II 51, 69–83.
594 Revill, A.T., Young, J.W., Lansdell, M., 2009. Stable isotopic evidence for trophic groupings and bio-
595 regionalization of predators and their prey in oceanic waters off eastern Australia. Mar. Biol.
596 156, 1241–1253.
597 Roberts, M., et al. (2013). Mechanics of dipole eddies in the western Mozambique Channel. Deep Sea
598 Res.Part II

599 Rubenstein, D.R., Hobson, K.A., 2004. From birds to butterflies: animal movement patterns and
600 stable isotopes. Trends Ecol. Evol. 19, 256–263.
601 Sabarros, P.S., Ménard, F., Lévénez, J., TewKai, E., Ternon, J., 2009. Mesoscale eddies influence
602 distribution and aggregation patterns of micronekton in the Mozambique Channel. Mar. Ecol.
603 Prog. Ser. 395, 101–107.
604 Schouten, M.W., de Ruijter, W.P.M., van Leeuwen, P.J., Ridderinkhof, H., 2003. Eddies and variability
605 in the Mozambique Channel. Deep-Sea Res. Part II 50, 1987–2003.
606 Seki, M.P., Polovina, J.J., Kobayashi, D.R., Bididgare R.R., Mitchum, G.T., 2002. An oceanographic
607 characterization of swordfish (Xiphias gladius) longline fishing grounds in the springtime
608 subtropical North Pacific. Fish. Ocean. 11, 251–266.
609 Sheldon, R.W., Sutcliffe, Jr., Paranjape, M.A., 1977. Structure of pelagic food chain and relationship
610 between plankton and fish production. J. Fish. Res. Board Can. 34, 2344-2353.
611 Stowasser, G., Atkinson, A., McGill, R.A.R., Phillips, R.A., Collins, M.A., Pond, D.W., 2012. Food web
612 dynamics in the Scotia Sea in summer: A stable isotope study. Deep Sea Res. Part II 59–60,
613 208–221.
614 Sweeting, C.J., Barry, J., Barnes, C., Polunin, N.V.C., Jennings, S., 2007. Effects of body size and
615 environment on diet-tissue [delta]15N fractionation in fishes. J. Exp. Mar. Biol. Ecol. 340, 1–
616 10.
617 Ternon, J.F., Barlow, R., Huggett, J., Kaehler, S., Marsac, F., Ménard, F., Potier, M., Roberts, M. (2013).
618 An overview of recent field experiments on the ecosystem's mesoscale signature in the
619 Mozambique Channel: from physics to upper trophic levels. Deep Sea Res. Part II
620 Tew Kai, E., Marsac, F., 2010. Influence of mesoscale eddies on spatial structuring of top predators'
621 communities in the Mozambique Channel. Prog. Ocean. 86, 214–223.
622 Tew-Kai, E., Marsac, F., 2009. Patterns of variability of sea surface chlorophyll in the Mozambique
623 Channel: A quantitative approach. J. Mar. Syst. 77, 77–88.
624 Torgersen, T., Kaartvedt, S., 2001. In situ swimming behaviour of individual mesopelagic fish studied
625 by split-beam echo target tracking. Ices J. Mar. Sci. 58, 346–354.
626 Vanderklift, M.A., Ponsard, S., 2003. Sources of variation in consumer-diet ?15N enrichment: a meta-
627 analysis. Oecologia 136, 169–182.
628 Venables, W.N., Ripley, B.D., 2002. Modern Applied Statistics with S, fourth ed., Springer, New York.
629 Waite, A.M., Muhling, B.A., Holl, C.M., Beckley, L.E., Montoya, J.P., Strzelecki, J., Thompson, P.A.,
630 Pesant, S., 2007. Food web structure in two counter-rotating eddies based on [delta]15N and
631 [delta]13C isotopic analyses: The Leeuwin Current and its Eddies. Deep Sea Res. Part II 54,
632 1055–1075.
633 Weimerskirch, H., Le Corre, M., Jaquemet, S., Potier, M., Marsac, F., 2004. Foraging strategy of a top
634 predator in tropical waters: great frigatebirds in the Mozambique Channel. Mar. Ecol. Prog.
635 Ser. 275, 297–308.
636 Young, J.W., Bradford, R., Lamb, T.D., Clementson, L.A., Kloser, R., Galea, H., 2001. Yellowfin tuna
637 (Thunnus albacares) aggregations along the shelf break off south-eastern Australia: links
638 between inshore and offshore processes. Mar. Freshw. Res. 52, 463–474.
639
640

641 Table 1. Body lengths and ranges (standard length for fishes, dorsal mantle length for squids,
642 cephalothorax length for crustaceans, total length for gelatinous organisms; in mm), $\delta^{13}C$
643 and $\delta^{15}N$ values (per mil), C/N ratios, and estimated trophic levels of micronekton from the
644 Mozambique Channel. Species or taxa are placed in broad class. Total number *n* and
645 numbers per Anticyclone, Cyclone, Divergence, Front, and Shelf are indicated. Values are
646 mean $\pm$ standard deviation. * indicates taxon for which body length effect was tested.
647
648 Table 2. Linear regression models fitted to $\delta^{15}N$ values (per mil) and body length (SL:
649 standard length in mm; DML: dorsal mantle length in mm) of four taxa of micronekton from
650 the Mozambique Channel. Models fitted to the squid *Ornithoteuthis volatilis*, and for the fish
651 taxa *Decapterus* sp., *Lestrolepis intermedia*, *Myctophum spinosum*, *Psenes* spp. and
652 *Symbolophorus evermanni* were not significant. Sample sizes and body length ranges
653 precluded model fitting for the remaining taxa.

654 Table 1

655

Broad class	Species	Phase	n	Body length mean (mm)	Body length range (mm)	$\delta^{13}C$	$\delta^{15}N$	C/N	TL	Anticyclone	Cyclone	Divergence	Front	Shelf
Gelatinous organisms	*Carinaria lamarckii*	adults	5	33.0	30-40	-19.7 ± 0.28	7.4 ± 0.61	3.4 ± 0.19	2.7 ± 0.2		5			
	Leptocephali larvae	larvae	10	217.6	170-260	-20.6 ± 0.57	5.8 ± 1.55	4.2 ± 0.37	2.2 ± 0.5		5			5
	Salpa maxima	solitary zooid	5	-	-	-19.4 ± 0.38	5.2 ± 0.11	4.1 ± 0.21	2				1	4
	Siphonophora		5	42.3	40-45	-19.3 ± 0.47	8.5 ± 0.63	3.2 ± 0.11	3.1 ± 0.2	3				2
Squids	*Cranchia scabra*	juveniles	9	40.1	35-47.1	-18.6 ± 0.49	9.4 ± 0.44	3.1 ± 0.21	3.3 ± 0.1	4	5			
	*Ornithoteuthis volatilis**	juveniles & adults	18	102.3	63.8-179	-18.5 ± 0.4	9.5 ± 0.8	3.1 ± 0.07	3.4 ± 0.2		1	7	5	5
	*Sthenoteuthis oualaniensis**	juveniles & adults	77	92.8	21.7-360	-18.2 ± 0.35	9.4 ± 0.77	3.1 ± 0.08	3.3 ± 0.2	19		38	14	6
Crustaceans	*Funchalia* spp.	adults	22	16.4	13.8-18.4	-18.6 ± 0.27	7.8 ± 0.8	3 ± 0.07	2.8 ± 0.3		8	3	7	4
	Oplophorus sp.	adults	8	13.0	12.7-13.5	-17.3 ± 0.24	9.3 ± 0.94	3 ± 0.04	3.3 ± 0.3		3		5	
	Oplophorus typus	adults	10	13.0	11.6-14.4	-18.1 ± 0.38	10.2 ± 0.32	3.3 ± 0.15	3.6 ± 0.1	5		5		
Fishes	*Argyropelecus aculeatus*	adults	23	56.8	42-77	-18.5 ± 0.46	10.5 ± 0.88	3.1 ± 0.08	3.7 ± 0.3		3	10	10	
	*Bramidae**	juveniles	6	82.2	43-152	-18.9 ± 0.61	9.2 ± 0.86	3.1 ± 0.03	3.3 ± 0.3		2	3	1	
	Bregmaceros macclellandii	adults	5	77.6	71-82	-18.6 ± 0.15	10.9 ± 0.44	3.1 ± 0.02	3.8 ± 0.1				5	
	Ceratoscopelus warmingii	adults	5	59.6	53-65	-18.9 ± 0.26	9.4 ± 0.57	3.1 ± 0.02	3.3 ± 0.2	5				
	*Cubiceps pauciradiatus**	juveniles & adults	55	98.1	23-140	-18.2 ± 0.4	9 ± 2.23	3.1 ± 0.06	3.2 ± 0.7		6	37	7	5
	Decapterus sp.*	juveniles	13	83.1	35-116	-18.5 ± 0.23	9.2 ± 2.23	3.1 ± 0.07	3.3 ± 0.7		10		3	
	Diaphus garmani	adults	5	56.2	40-75	-18.4 ± 0.35	10.4 ± 0.94	3.3 ± 0.03	3.7 ± 0.3				5	
	Diaphus metopoclampus	adults	6	57.7	54-62	-19.3 ± 0.19	12.1 ± 0.44	3.3 ± 0.04	4.2 ± 0.1			5	1	
	Diaphus richardsoni	adults	39	47.0	36-59	-18.9 ± 0.23	10.8 ± 0.52	3.2 ± 0.1	3.8 ± 0.2	5			14	20
	Diaphus spp.	adults	16	62.7	50-80	-18.5 ± 0.29	10.5 ± 0.62	3.1 ± 0.04	3.7 ± 0.2	5			5	6
	Gonostoma elongatum	juveniles & adults	5	108.8	96-120	-18.9 ± 0.12	9.7 ± 0.39	3 ± 0.02	3.4 ± 0.1			5		
	Gymnoscopelus sp.	adults	5	68.6	60-76	-18.6 ± 0.19	10.2 ± 0.38	3.1 ± 0.02	3.6 ± 0.1				5	
	Hygophum hygomii	adults	15	52.1	37.3-62	-18.8 ± 0.2	9.9 ± 0.66	3.1 ± 0.02	3.5 ± 0.2	5	5	1	4	
	*Lestrolepis intermedia**	juveniles & adults	17	127.1	75-171	-18.8 ± 0.48	9.7 ± 0.83	3.2 ± 0.09	3.4 ± 0.3		2	4	3	8
	Lobianchia gemellarii	adults	5	50.0	45-70	-18.4 ± 0.18	11.1 ± 0.73	3.1 ± 0.01	3.9 ± 0.2		1			4
	*Myctophum spinosum**	juveniles & adults	33	65.7	40-86	-18.8 ± 0.24	8.9 ± 0.38	3.2 ± 0.05	3.2 ± 0.1	2		16	10	5
	Psenes spp.*	juveniles	8	47.4	36-76	-19.2 ± 0.65	7.6 ± 0.34	3.2 ± 0.24	2.8 ± 0.1	2	6			
	Pterycombus petersii	juveniles	5	58.2	35-77	-19.6 ± 0.2	8.2 ± 0.66	3 ± 0.03	2.9 ± 0.2		3	2		
	Scopelosaurus hoedti	adults	6	123.7	112-126	-18.9 ± 0.04	11.4 ± 0.33	3.1 ± 0.01	3.9 ± 0.1		1			5
	*Symbolophorus evermanni**	adults	57	77.4	42-108	-18.6 ± 0.24	9.3 ± 0.69	3.2 ± 0.07	3.3 ± 0.2	5		30	12	10
	Thunnus spp.*	juveniles	33	43.0	23-84	-18.3 ± 0.51	7 ± 0.8	3.1 ± 0.06	2.6 ± 0.2	8	6	16		3
	Vinciguerria nimbaria	adults	14	39.9	32-46	-18.8 ± 0.29	10 ± 0.43	3.1 ± 0.03	3.5 ± 0.1		5	5	4	

656

657 Table 2

Taxon	Regression equation	r^2 (%)	*p*	*n*
Bramidae	$\delta^{15}N = 7.77 + 0.0179 \times SL$	87.4	0.006	6
Thunnus spp.	$\delta^{15}N = 6.05 + 0.0226 \times SL$	19.9	0.01	33
Sthenoteuthis oualaniensis	$\delta^{15}N = 8.27 + 0.0122 \times DML$	46.4	< 0.0001	76
Cubiceps pauciradiatus (not Cyclone)	$\delta^{15}N = 6.04 + 0.0242 \times SL$	90.24	< 0.0001	6
Cubiceps pauciradiatus (Cyclone)	$\delta^{15}N = 11.80 + 0.0242 \times SL$			49

658

659

660 Fig. 1. Map showing the 34 sampling stations carried out in 2008 (cruise MC08) and 2009
661 (cruise MC09B) in the Mozambique Channel. Stations are categorized according to
662 mesoscale features (no cyclone was sampled in MC08A).
663
664 Fig. 2. Summary of $\delta^{13}C$ and $\delta^{15}N$ isotope signatures (mean $\pm$ standard deviation in per mil)
665 of micronekton taxa sampled in the Mozambique Channel. Set diagrams group the four
666 broad categories (fishes, squids, crustaceans and gelatinous organisms).
667
668 Fig. 3. $\delta^{15}N$ (a) and $\delta^{13}C$ (b) isotope signatures (mean $\pm$ standard deviation in per mil) of
669 micronekton taxa sampled in the Mozambique Channel. Taxa are placed in broad class and
670 then isotope signatures of both nitrogen and carbon are sorted in order of decreasing
671 depletion.
672
673 Fig. 4. Pruned regression tree that predicts the $\delta^{15}N$ signatures of five groups of micronekton
674 organisms. Each terminal node is characterized by $\delta^{15}N$ value (per mil), number of
675 individuals, corresponding taxa and mesoscale feature (A – Anticyclonic, C – Cyclonic, D –
676 Divergence, F – Frontal, S – Shelf). Covariates used to develop the tree are taxon and
677 mesoscale features.
678
679 Fig. 5. Pruned regression tree that predicts the $\delta^{13}C$ signatures of four groups of micronekton
680 organisms. Each terminal node is characterized by $\delta^{13}C$ value (per mil), number of
681 individuals, corresponding taxa and mesoscale feature (A – Anticyclonic, C – Cyclonic, D –
682 Divergence, F – Frontal, S – Shelf). Covariate used to develop the tree is taxon.
683

684 Fig. 6. δ^{15}N values (per mil) from (a) Bramidae (b) *Sthenoteuthis oualaniensis* (c) *Cubiceps*
685 *pauciradiatus* (d) *Thunnus* spp. plotted versus body length (standard length in mm for (a), (c)
686 and (d); dorsal mantle length in mm for (b)). Simple linear regressions for δ^{15}N values versus
687 body length are plotted (see text and Table 2).

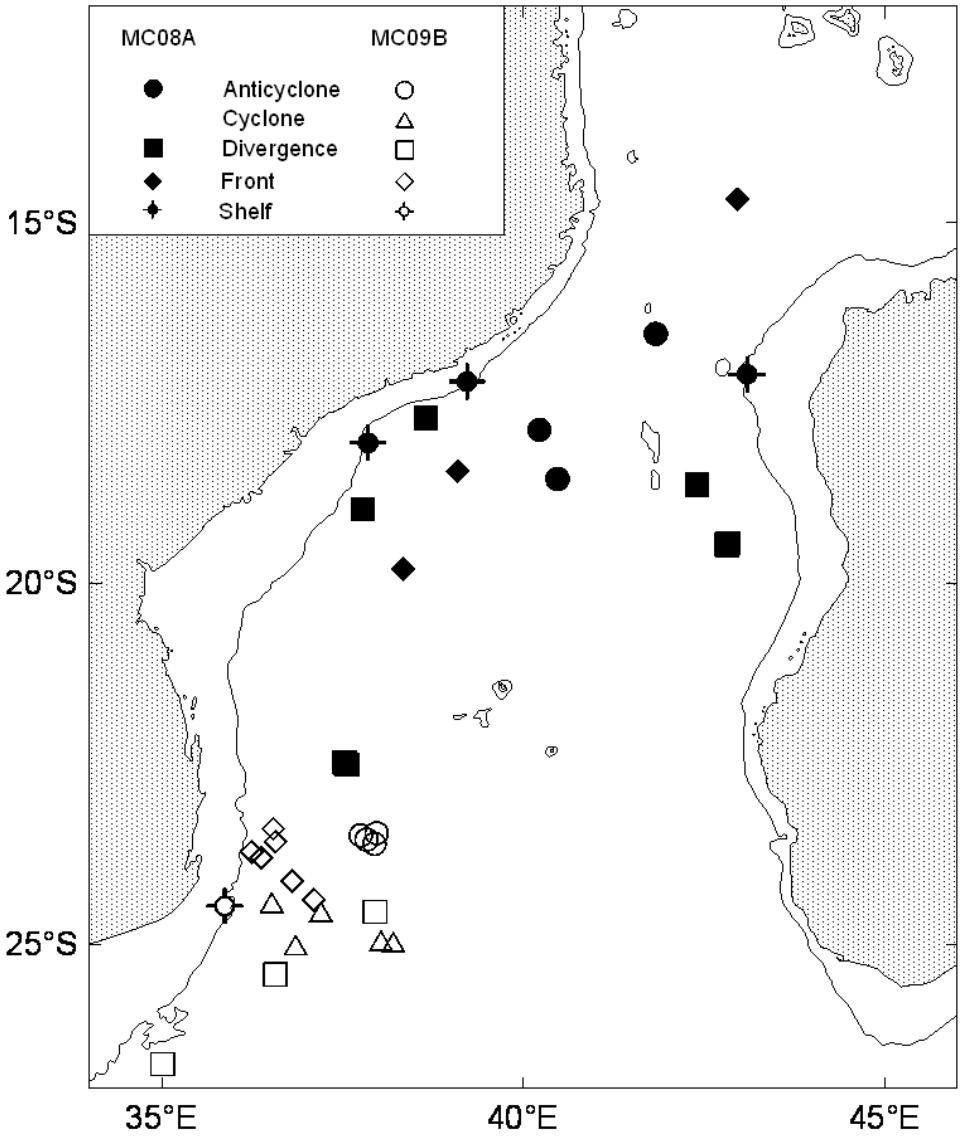
MC08A
MC09B
Anticyclone
Cyclone
Divergence
Front
Shelf
15°S
20°S
25°S
35°E
40°E
45°E

688

689 Fig.1

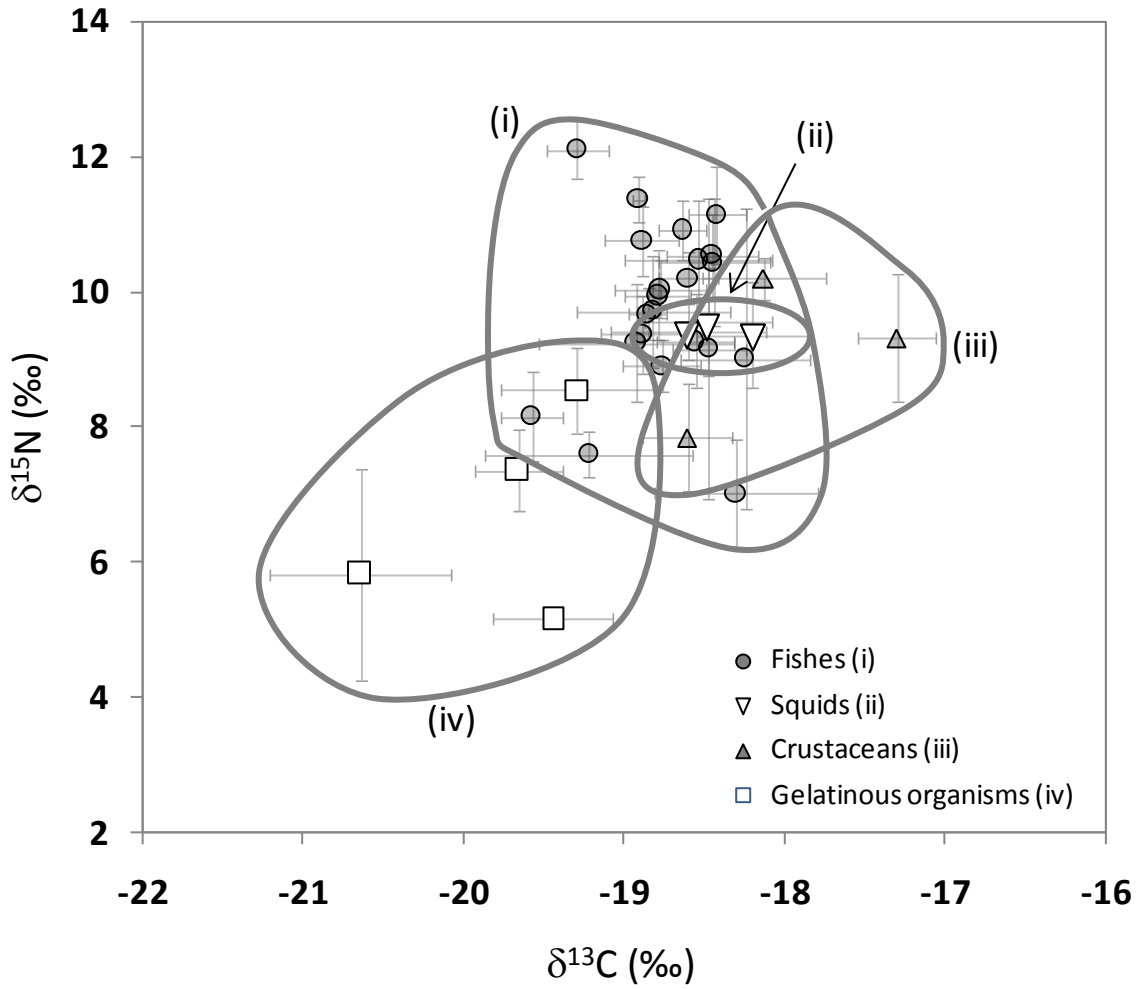
14
12
10
8
6
4
2
-22
-21
-20
-19
-18
-17
-16
δ15N (‰)
δ13C (‰)
(i)
(ii)
(iii)
(iv)
Fishes (i)
Squids (ii)
Crustaceans (iii)
Gelatinous organisms (iv)

690

691 Fig. 2

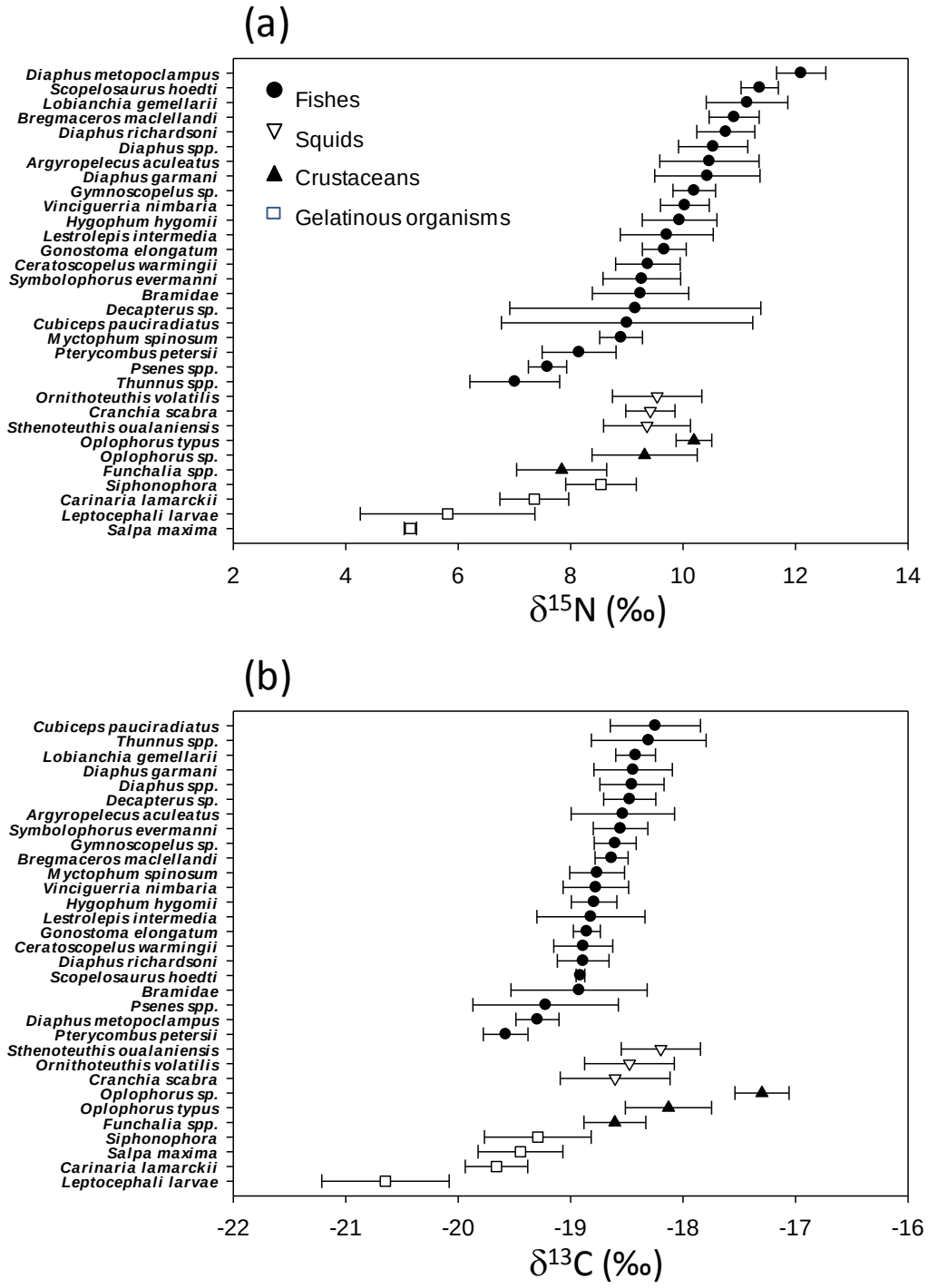
(a)
Diaphus metopoclampus
Scopelosaurus hoedti
Lobianchia gemellarii
Bregmaceros maclellandi
Diaphus richardsoni
Diaphus spp.
Argyropelecus aculeatus
Diaphus garmani
Gymnoscopelus sp.
Vinciguerria nimbaria
Hygophum hygomii
Lestrolepis intermedia
Gonostoma elongatum
Ceratoscopelus warmingii
Symbolophorus evermanni
Bramidae
Decapterus sp.
Cubiceps pauciradiatus
Myctophum spinosum
Pterycombus petersii
Psenes spp.
Thunnus spp.
Ornithoteuthis volatilis
Cranchia scabra
Sthenoteuthis oualaniensis
Oplophorus typus
Oplophorus sp.
Funchalia spp.
Siphonophora
Carinaria lamarckii
Leptocephali larvae
Salpa maxima
Fishes
Squids
Crustaceans
Gelatinous organisms
2
4
6
8
10
12
14
δ15N (‰)
(b)
Cubiceps pauciradiatus
Thunnus spp.
Lobianchia gemellarii
Diaphus garmani
Diaphus spp.
Decapterus sp.
Argyropelecus aculeatus
Symbolophorus evermanni
Gymnoscopelus sp.
Bregmaceros maclellandi
Myctophum spinosum
Vinciguerria nimbaria
Hygophum hygomii
Lestrolepis intermedia
Gonostoma elongatum
Ceratoscopelus warmingii
Diaphus richardsoni
Scopelosaurus hoedti
Bramidae
Psenes spp.
Diaphus metopoclampus
Pterycombus petersii
Sthenoteuthis oualaniensis
Ornithoteuthis volatilis
Cranchia scabra
Oplophorus sp.
Oplophorus typus
Funchalia spp.
Siphonophora
Salpa maxima
Carinaria lamarckii
Leptocephali larvae
-22
-21
-20
-19
-18
-17
-16
δ13C (‰)

692

693 Fig.3

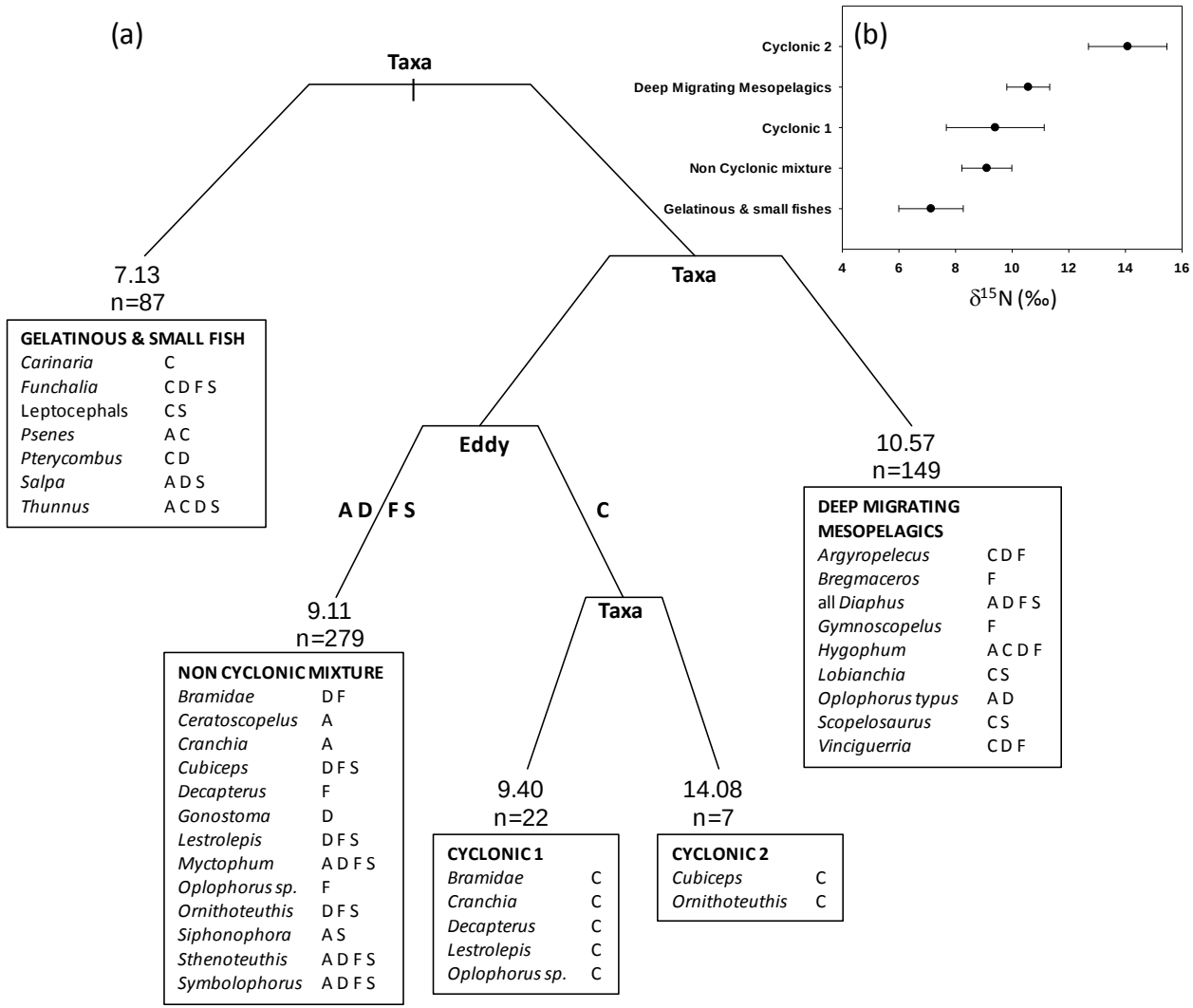
(a)
Taxa
7.13
n=87
GELATINOUS & SMALL FISH
Carinaria C
Funchalia C D F S
Leptocephals C S
Psenes A C
Pterycombus C D
Salpa A D S
Thunnus A C D S
Taxa
Eddy
A D F S
C
10.57
n=149
DEEP MIGRATING MESOPELAGICS
Argyropelecus C D F
Bregmaceros F
all Diaphus A D F S
Gymnoscopelus F
Hygophum A C D F
Lobianchia C S
Oplophorus typus A D
Scopelosaurus C S
Vinciguerria C D F
9.11
n=279
NON CYCLONIC MIXTURE
Bramidae D F
Ceratoscopelus A
Cranchia A
Cubiceps D F S
Decapterus F
Gonostoma D
Lestrolepis D F S
Myctophum A D F S
Oplophorus sp. F
Ornithoteuthis D F S
Siphonophora A S
Sthenoteuthis A D F S
Symbolophorus A D F S
Taxa
9.40
n=22
CYCLONIC 1
Bramidae C
Cranchia C
Decapterus C
Lestrolepis C
Oplophorus sp. C
14.08
n=7
CYCLONIC 2
Cubiceps C
Ornithoteuthis C
(b)
Cyclonic 2
Deep Migrating Mesopelagics
Cyclonic 1
Non Cyclonic mixture
Gelatinous & small fishes
4
6
8
10
12
14
16
δ15N (‰)

694

695 Fig.4

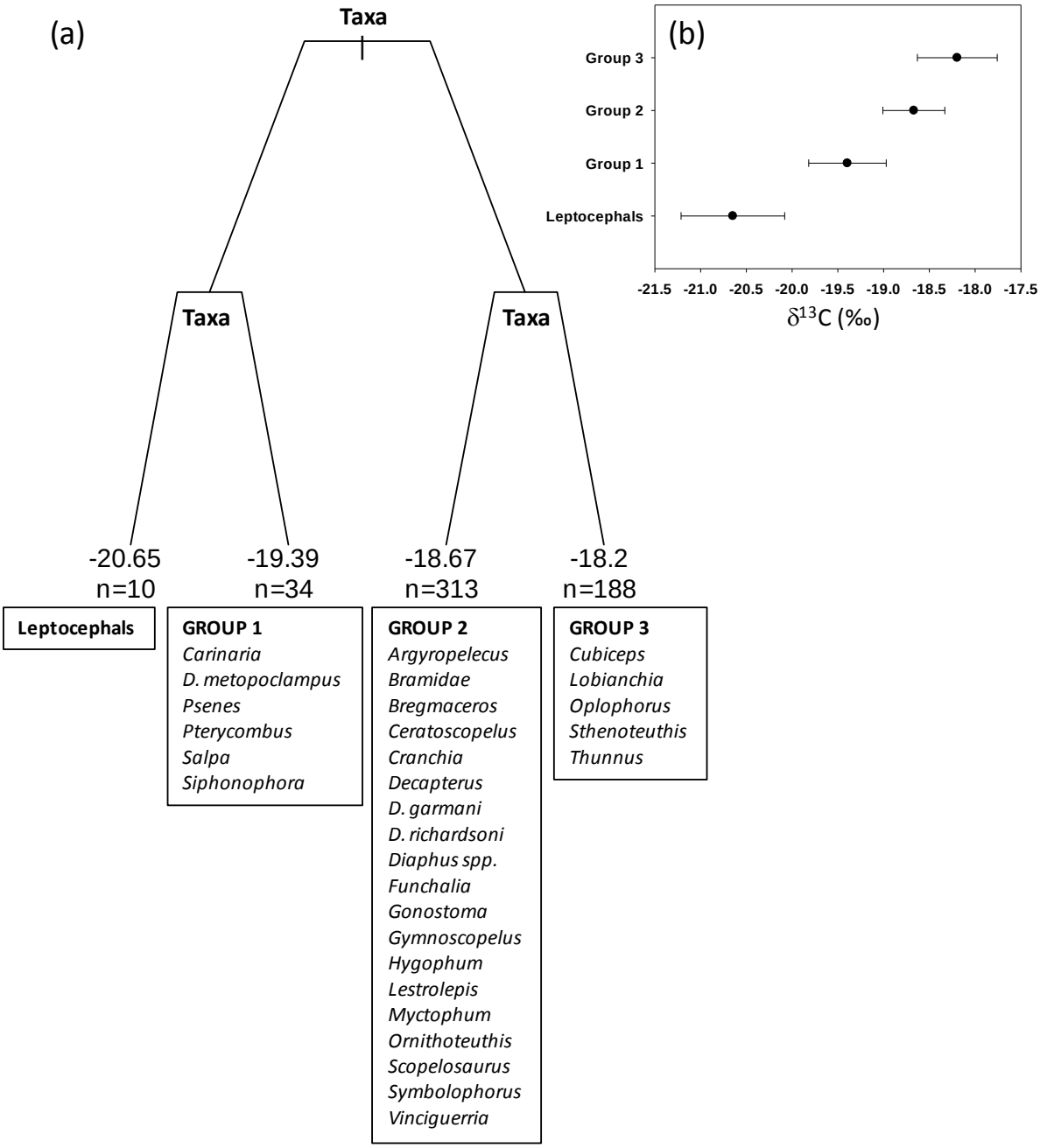
(a)
Taxa
Taxa
Taxa
-20.65
n=10
-19.39
n=34
-18.67
n=313
-18.2
n=188
Leptocephals
GROUP 1
Carinaria
D. metopoclampus
Psenes
Pterycombus
Salpa
Siphonophora
GROUP 2
Argyropelecus
Bramidae
Bregmaceros
Ceratoscopelus
Cranchia
Decapterus
D. garmani
D. richardsoni
Diaphus spp.
Funchalia
Gonostoma
Gymnoscopelus
Hygophum
Lestrolepis
Myctophum
Ornithoteuthis
Scopelosaurus
Symbolophorus
Vinciguerria
GROUP 3
Cubiceps
Lobianchia
Oplophorus
Sthenoteuthis
Thunnus
(b)
Group 3
Group 2
Group 1
Leptocephals
-21.5 -21.0 -20.5 -20.0 -19.5 -19.0 -18.5 -18.0 -17.5
δ13C (‰)

696

697 Fig. 5

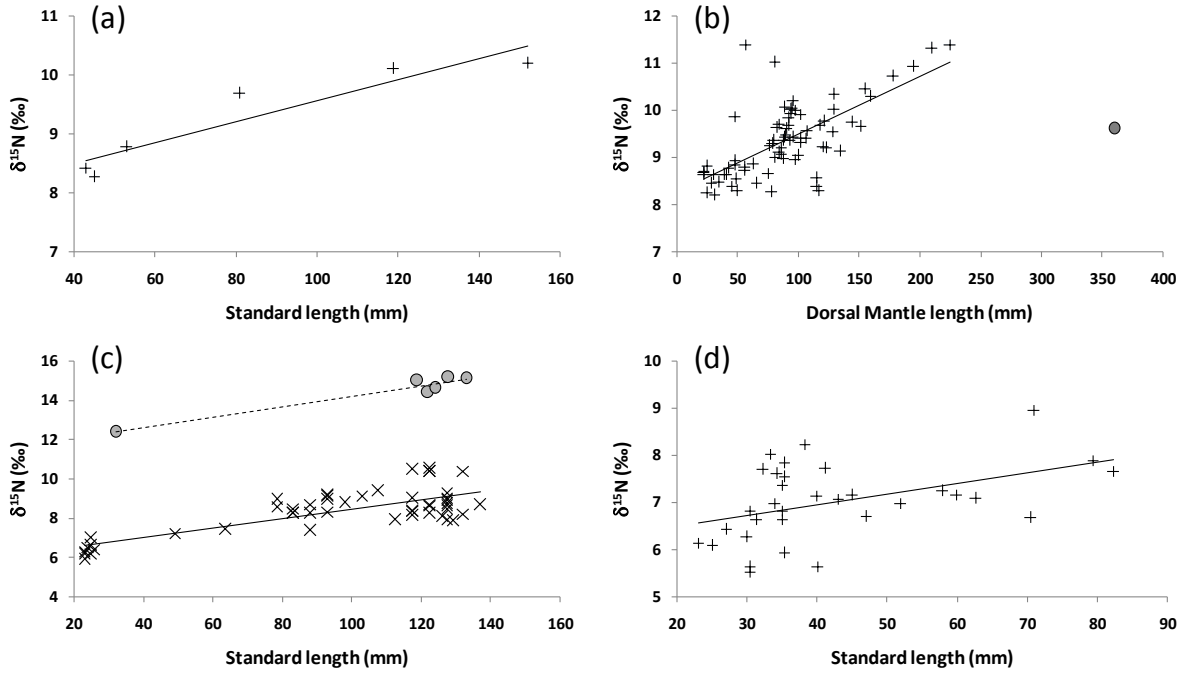
(a)
δ15N (‰)
Standard length (mm)
(b)
δ15N (‰)
Dorsal Mantle length (mm)
(c)
δ15N (‰)
Standard length (mm)
(d)
δ15N (‰)
Standard length (mm)

698

699 Fig.6